

# In Situ synthesis of Ceramic Composite Materials in the Ti–B–C–N System by a Mechanically induced Self-Sustaining Reaction

Miguel A. Avilés, Ernesto Chicardi, José M. Córdoba, María J. Sayagués, and Francisco J. Gotor†

Instituto de Ciencia de Materiales de Sevilla (CSIC-US), Américo Vespucio 49, 41092 Sevilla, Spain

The synthesis of multicomponent ceramic materials in the titanium-diboride-carbide-nitride-carbonitride system by the mechanochemical process known as the mechanically induced self-sustaining reaction (MSR) was investigated. Ceramic composite powders containing  $\text{TiB}_2$  and TiC, TiN or  $\text{TiC}_x\text{N}_{1-x}$  were prepared from a blended mixture of the elements by exploiting the highly exothermic nature of the formation reactions. The synthesis of the composite materials was made possible by the ability of the MSR to simultaneously induce independent self-sustaining reactions, generating a mixture of ceramic phases. The composition of the ceramic composites was designed using the initial atomic ratio of the reactants, and the achieved microstructure was characterized by  $\text{TiB}_2$  particles in the micrometric range, surrounded by submicrometric and nanometric TiC, TiN, or  $\text{TiC}_x\text{N}_{1-x}$  crystals.

## I. Introduction

CERAMIC materials in the Ti–B–C–N system are interesting because single phases, such as  $\text{TiB}_2$ , TiC, TiN, and  $\text{TiC}_x\text{N}_{1-x}$  solid solutions, have excellent mechanical, thermal, and electrical properties, which make them very useful for structural applications.<sup>1–4</sup> It has been reported that ceramic composites obtained within these phases possess superior mechanical properties (hardness, wear resistance, and fracture toughness) compared with their constituent ceramic components.<sup>5</sup> Moreover, due to an excellent combination of mechanical, wear, and electrical properties as well as good corrosion resistance, some of these composites, such as  $\text{TiB}_2$ –TiN and  $\text{TiB}_2$ –TiC, are candidate materials for high-technology applications, in which the operating conditions can be defined as severe.<sup>6</sup> In addition, their use in other nonstructural applications, such as molten-metal crucibles, cathodes in aluminum electro-melting, and vaporizing elements in vacuum-metal deposition installations, have also been studied.<sup>7,8</sup> Furthermore, compared with conventional cermets based on WC and TiC, cermets based on  $\text{TiC}_x\text{N}_{1-x}$ – $\text{TiB}_2$  composites exhibit a higher hardness and chemical stability at high temperatures and are good alternatives for wear-resistant materials.<sup>9</sup> In this framework, ceramic composites in the Ti–B–C–N system represent promising materials for applications as wear-resistant parts and in high-performance cutting tools and also exhibit good behavior as high-temperature structural components in heat exchangers and engines.<sup>10–12</sup>

Usually, TiN, TiC,  $\text{TiC}_x\text{N}_{1-x}$ , and  $\text{TiB}_2$  powders are produced by reduction processes (carbothermal or borothermal

reduction) featuring titania in a controlled atmosphere.<sup>13–15</sup> However, the appearance of secondary phases, such as  $\text{TiO}_2$ ,  $\text{Ti}_x\text{O}_y\text{C}$ , and  $\text{TiBO}_3$ , in the final product lowers the purity of the powders produced from the reduction reaction. In recent years, self-propagating high-temperature synthesis (SHS), which has the advantages of time and energy efficiency, has been a promising route for the production of advanced materials, including borides, carbides, nitrides, and carbonitrides.<sup>16–19</sup> The mechanochemical process referred to as the mechanically induced self-sustaining reaction (MSR) is similar to thermally ignited SHS and requires highly exothermic chemical reactions.<sup>20</sup> The MSR has proved to be adequate in producing  $\text{TiB}_2$ , TiC, and Ti(C,N) from mixtures of elemental titanium with boron or carbon in an inert or nitrogen atmosphere.<sup>21–23</sup> In addition, MSR has allowed for the production of nanocrystalline carbonitride powders with homogeneous and controlled chemical compositions by adequately adjusting the milling parameters and the metal-to-carbon atomic ratio in the starting mixture.<sup>23</sup>

$\text{TiB}_2$ –TiN,  $\text{TiB}_2$ –TiC, and  $\text{TiB}_2$ – $\text{TiC}_x\text{N}_{1-x}$  ceramic composites are traditionally prepared from the premixed powders of single-phase components. Recently, research attention has turned to the reactive *in situ* synthesis of these ceramic composites, which has usually been performed by SHS or other related combustion methods.<sup>24–27</sup> The reactants commonly used in these studies are elemental Ti and  $\text{B}_4\text{C}$  and BN powders as the sole source of B, C, and N, which unfortunately fix the final composition of the ceramic composite. To extend the range of compositions available through these methods, the addition of elemental B and C to the reactant mixture and the use of a nitrogen atmosphere instead of an inert one have been proposed.<sup>28–31</sup> Moreover, only few works have reported the synthesis of these composites by milling processes in which relatively long milling periods were always necessary.<sup>32–34</sup> Longer milling times were required when BN and  $\text{B}_4\text{C}$  rather than elemental mixtures were used as reactants, and a subsequent thermal treatment was often compulsory to achieve full conversion.<sup>35,36</sup>

The MSR is a simple, fast, and direct method and, in contrast to SHS, requires only a single step to mix the reactants, produce the product, and promote its subsequent homogenization. Thus, in this study, we intended to prepare different ceramic composites in the Ti–B–C–N system by performing simultaneous MSR processes from mixtures of elements in a controlled atmosphere. We report that the MSR is suitable for obtaining composite materials because excellent powder homogeneity and a fine microstructure can be simultaneously achieved.

## II. Experimental Procedure

Titanium powder (99% purity, <325 mesh; Strem Chemicals, Newburyport, MA), boron powder (95%–97% purity, amorphous powder; Fluka, St. Louis, MO), and graphite powder (11 m<sup>2</sup>/g, Fe ≤ 0.4%; Merck, Whitehouse Station, NJ) were used in this work. The different powder mixtures were ball milled under 6 bars of high-purity helium gas ( $\text{H}_2\text{O}$  < 3 ppm,

R. Cutler—contributing editor

Manuscript No. 30754. Received December 02, 2011; approved February 22, 2012. Supported by the Spanish government under grant No. MAT2010-17046, which was financed in part by the European Regional Development Fund 2007-2013. E. Chicardi and J. M. Córdoba were supported by CSIC through JAE-Pre and JAE-Doc grants, respectively, financed in part by the European Social Fund (ESF).

†Author to whom correspondence should be addressed. e-mail: fgotor@cica.es

$O_2 < 2$  ppm and  $C_nH_m < 0.5$  ppm; Air Liquide España, S. A., Madrid, Spain) or nitrogen gas ( $H_2O$  and  $O_2 < 3$  ppm; Air Liquide España) using a modified planetary ball mill (model Micro Mill Pulverisette 7; Fritsch, Idar-Oberstein, Germany) operated at a constant gas pressure; self-propagating reactions were detected during milling. These reactions were detected by connecting the vial to a gas cylinder via a rotating union (model 1005-163-038; Deublin, Waukegan, IL) and to a flexible polyamide tube and continuously monitoring the gas pressure with an SMC solenoid valve (model EVT307-5DO-01F-Q; SMC Co., Tokyo, Japan) connected to an ADAM-4000 series data acquisition system (Esis Pty Ltd., Pennant Hills, Australia). When the self-sustaining reaction occurs, the increase in temperature due to the exothermic reaction produces an instantaneous increase in the total pressure. The ignition time ( $t_{ig}$ ) for each mixture, e.g., the milling time required to ignite the reactant mixture, was obtained from the spike observed in the time-pressure record. After ignition, the milling was prolonged for 30 min to ensure full conversion and to obtain a homogeneous product.

All milling experiments were performed under the same experimental conditions. Five grams of powder, together with seven tempered steel balls, were placed in a 45-mL tempered steel vial (67 Rc). The diameter and weight of balls were 15 mm and 12.39 g, respectively. The powder-to-ball mass ratio (PBR) was 1/17.35. The vial was purged several times, and the desired gas pressure was selected before milling. A spinning rate of 600 rpm for both the rotation of the supporting disk and the superimposed rotation in the direction opposite to that of the vial rotation was used.

X-ray diffraction (XRD) analysis of the resultant ceramic composite powders was performed on a X'Pert Pro MPD diffractometer (Panalytical, Almelo, the Netherlands) equipped with a graphite diffracted beam monochromator and a solid-state detector (X'Cellerator), with an angular aperture of  $2.12^\circ$  ( $2\theta$ ), using  $CuK\alpha$  radiation (45 kV, 40 mA) over a  $2\theta$ -range of  $20$ – $150^\circ$  and a step size of  $0.017^\circ$ , with a counting time of 300 s/step. Using the freely distributed program FULLPROF,<sup>37</sup> the Rietveld refinement method was employed for the quantitative phase analysis of composite products.

The morphology of the samples was characterized by scanning electron microscopy (SEM) using a FEG S-4800 microscope (Hitachi High-Tech, Tokyo, Japan). Transmission electron microscopy (TEM), electron diffraction (ED), and electron energy loss spectroscopy (EELS) were performed using a CM-200 microscope (FEI, Hillsboro, OR) operating at 200 kV, with a  $LaB_6$  filament (point resolution 2.3 Å), a double-tilt goniometer, and a Peels spectrometer. EELS spectra were acquired using a Gatan model 766-2K parallel detection electron spectrometer (Gatan, Inc., Pleasanton, CA) and were recorded in the diffraction mode at a collection angle of 1.45 mrad. The measured energy resolution at the zero-loss peak of the coupled microscope/spectrometer system was  $\sim 2$  eV. A low-loss spectrum was also recorded with each edge in the same illuminated area. After background subtraction with a standard power-law function, the

spectra were deconvoluted for plural scattering with the Fourier-ratio method, and semi-quantitative analyses were performed. All of these treatments were performed within the EL/P program (Gatan).

### III. Results and Discussion

Table I shows different elemental mixtures submitted to milling to obtain ceramic composite materials belonging to the Ti–B–C–N system by the MSR process. To provide insight into the MSR process leading to these ceramic composites,  $TiB_2$ , TiC, and  $TiC_xN_{1-x}$  monophasic products were also obtained by the same procedure. For all mixtures, the time-pressure record showed a single MSR effect, and the ignition times ( $t_{ig}$ ) are shown in Table I. The products obtained after the MSR processes were identified by XRD, and the observed phases are also depicted in Table I. The XRD diagrams corresponding to the three ceramic composite products (samples TBN, TBC, and TBCN) are shown in Fig. 1. Samples TBC and TBCN were constituted by a biphasic product featuring  $TiB_2/TiC$  and  $TiB_2/TiC_xN_{1-x}$ , respectively, whereas sample TBN was composed of three distinct phases ( $TiB_2$  and TiN as the main phases and TiB as a minority phase). In the case of samples TB, TC, and TBC, the syntheses of which were performed in a helium environment, only solid-state reactions were induced during milling; however, in the production of samples TCN, TBN, and TBCN, nitrogen acted as a reagent gas and was incorporated into the product, leading to more complex reactions.

In Table I, the ratio of the reaction heat of formation and the room temperature heat capacity of the products ( $\Delta H_{298}^0/Cp_{298}$ )<sup>38</sup> is also shown for each sample. This is a useful parameter that correlates closely with the adiabatic temperature and provides information regarding the ignition capacity of a reactant mixture.<sup>20</sup> In all cases, this parameter was well above the 2000K value that is regarded as a necessary criterion to conduct the MSR process. For samples TB, TC, and TBC, for which solid-state reactions were performed, an expected inverse correlation between  $\Delta H_{298}^0/Cp_{298}$  and  $t_{ig}$  was observed with a decrease in ignition time as the exothermic character of the process increased. Although the presence of nitrogen increased the exothermic character of the mixtures, the ignition times for samples TCN, TBN, and TBCN were not proportionally reduced. A direct relationship between  $\Delta H_{298}^0/Cp_{298}$  and  $t_{ig}$  was observed, and the ignition time increased with the relative amount of nitrogen with respect to the solid reactants in the associated reaction. This was a direct consequence of the fact that MSR processes are more difficult to induce when solid-gas reactions are involved than when only solid phases are used.

In the literature,<sup>26,31</sup> it has been reported that the initiation of SHS reactions in the Ti–B–C–N system is controlled by the rate of the surface reaction among the reagents, and is essential for the propagation of the combustion wave and to achieve full conversion to reach the formation temperature of a Ti-containing eutectic melt; this facilitates the contact between the reactants. It is for this reason that, to assist the

**Table I.** Elemental Mixtures Submitted to Milling in the Ti–B–C–N System, Indicating the Initial Atomic Ratio of the Reactants, the Atmosphere Used, the Ignition Time ( $t_{ig}$ ) of the MSR Process, the  $\Delta H_{298}^0/Cp_{298}$  Ratio as a Measurement of the Self-Sustaining Capacity of the Mixture, and the Obtained Products, as Identified by XRD.

Sample	Solid Reactants (atomic ratio)	Atmosphere	$t_{ig}$ (min)	$\Delta H_{298}^0/Cp_{298}$ (K) <sup>39</sup>	Products
TB	Ti + B (1/2)	He	32	6214	$TiB_2$
TC	Ti + C (1/1)	He	62	5427	TiC
TCN	Ti + C (1/0.5)	$N_2$	72	7357	$TiC_xN_{1-x}$
TBN	Ti + B (1/1)	$N_2$	57	6911	$TiB_2$ + TiN + TiB <sup>†</sup>
TBC	Ti + B + C (2/2/1)	He	55	5820	$TiB_2$ + TiC
TBCN	Ti + B + C (2/2/0.5)	$N_2$	44	6785	$TiB_2$ + $TiC_xN_{1-x}$

<sup>†</sup>minor phase.

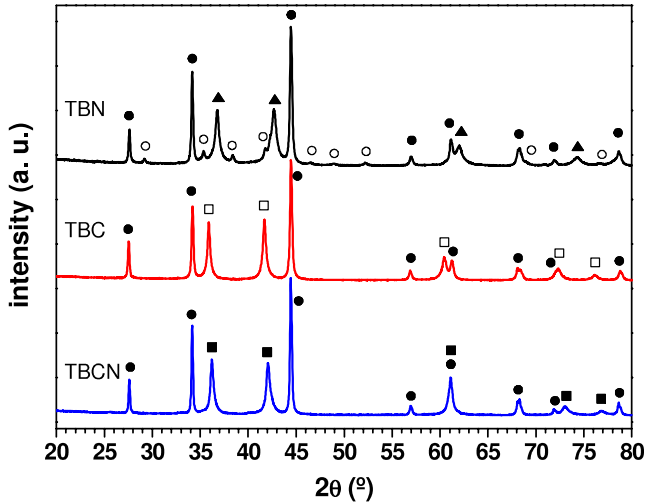


**Fig. 1.** X-ray powder diffraction diagrams of products obtained from the MSR process for samples TBN, TBC, and TBCN. (●)  $\text{TiB}_2$ ; (■)  $\text{TiC}_x\text{N}_{1-x}$ ; (□) TiC; (▲) TiN; (○) TiB.

self-sustaining reaction, the addition of Ni to the reactant mixture has been proposed to promote the formation of a Ti–Ni eutectic melt at a lower temperature at which the reactants are dissolved and the final product is precipitated.<sup>31,39</sup> The MSR process affords the advantage of extremely intimate mixing of reagents; moreover, when the reaction is ignited, it spreads quickly throughout the entire sample, completely transforming the reactants into products.

It is worth noting that in samples TBN, TBC, and TBCN, the different phases constituting the composite products were actually formed through independent self-sustaining reactions. The fact that only a single combustion process was detected in the time-pressure record suggests that these independent reactions occurred simultaneously. It can be observed in Table I that sample TB (Ti + B) reacted after 32 min of milling treatment in a He atmosphere, while sample TC (Ti + C) ignited at 62 min, requiring a greater extent of activation. However, in sample TBC (Ti + B + C), which can be seen as the TB and TC collection, carbon first prevented the reaction between titanium and boron, delaying the ignition; however, when it occurred after 55 min of milling, the heat released by this reaction triggered the reaction between titanium and carbon, creating a unique propagation front that caused the consumption of all the reactants, which were instantly transformed into  $\text{TiB}_2$  and TiC. It is for this reason that two different MSR events were not detected; instead, only one event corresponding to these two simultaneous formation reactions was observed. This same explanation can be extended to sample TBCN, which is a collection of samples TB and TCN.

For sample TBN, the aim of the reactant mixture was to obtain an equimolar  $\text{TiB}_2/\text{TiN}$  product through the multiple reaction  $2\text{Ti} + 2\text{B} + 1/2\text{N}_2 = \text{TiB}_2 + \text{TiN}$  such that the heat released during the formation of  $\text{TiB}_2$  would promote the self-sustaining reaction between the exceeding Ti and nitrogen gas. However, despite the fact that the reaction between titanium and nitrogen (a reactant gas) is extremely exothermic ( $\Delta H_{298}^0/C_{p298} = 9129$  K), its induction by a milling process is more difficult to achieve than the reaction between titanium and boron or carbon (solid reactants). This was evidenced by the fact that the attempted self-sustaining reaction of titanium with gaseous nitrogen, under the same milling conditions used in the present work and without any other element, was not detected after several hours of treatment. The combustion synthesis of TiN induced by the high-energy ball milling of Ti under a nitrogen atmosphere has already been reported, although only after prolonged treatment in an extremely intensive milling regime.<sup>40</sup> Therefore, the existence

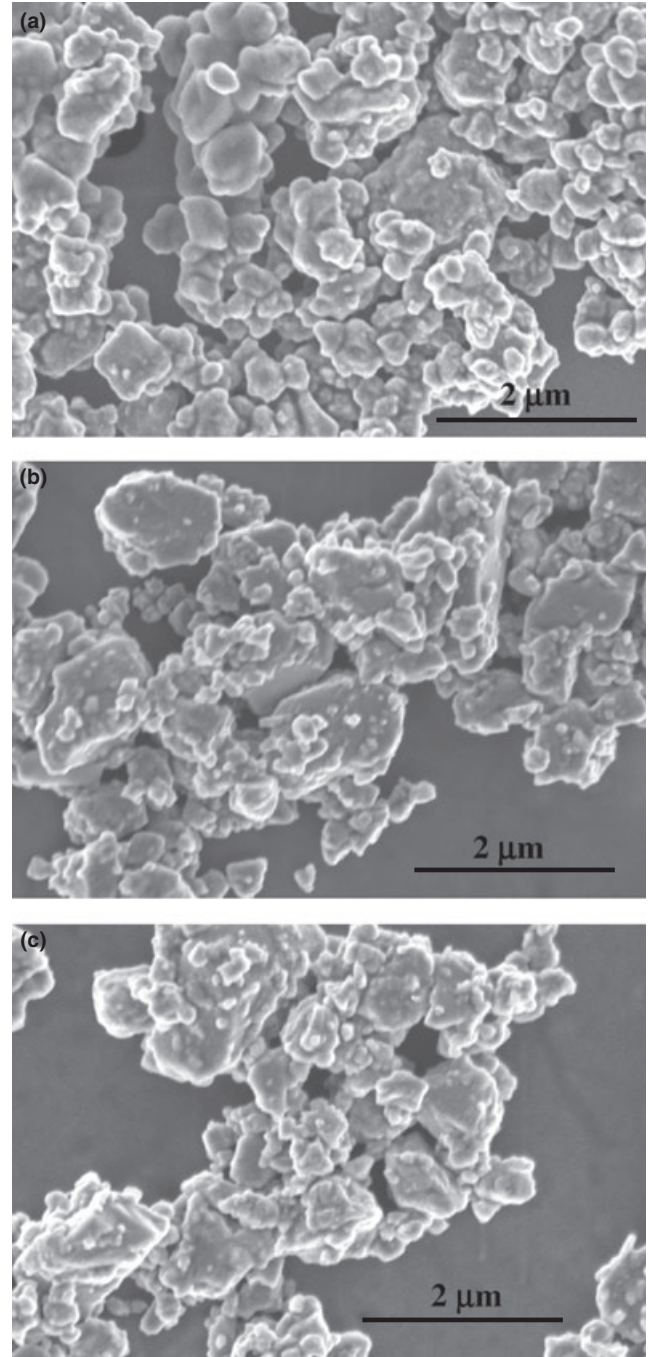


**Fig. 2.** SEM micrographs obtained for the (a) TBN, (b) TBC and (c) TBCN ceramic composites.

of TiB in sample TBN as a minor phase was the result of a limited absorption of nitrogen by the sample (incomplete reaction between Ti and  $\text{N}_2$ ); this prevented the formation of the intended  $\text{TiB}_2/\text{TiN}$  mixture but allowed for the consumption of all of the elemental Ti, which was not detected in the final product.

The microstructural characterization of the three ceramic composite powders (TBN, TBC, and TBCN) was performed using scanning and transmission electron microscopy techniques (SEM, TEM, ED and EELS), and the representative results are presented in Figs 2–4. SEM micrographs (Fig. 2) show the morphology and particle size distribution of the three samples. As can be observed, all the materials were quite similar and were formed by large faceted particles (0.5–2  $\mu\text{m}$ ) surrounded by smaller rounded ones (0.1–0.3  $\mu\text{m}$ ). The EDX analysis did not provide valuable information because B, C, and N have very low atomic masses.

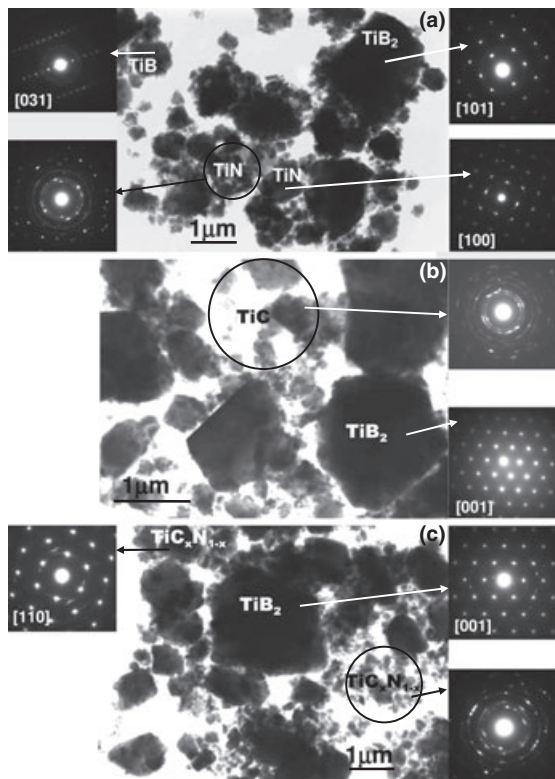


Fig. 3. TEM and ED representative results obtained for (a) TBN, (b) TBC, and (c) TBCN composites.  $\text{TiB}_2$ ,  $\text{TiB}$ ,  $\text{TiN}$ ,  $\text{TiC}$ , and  $\text{TiC}_x\text{N}_{1-x}$  phases are marked in the images.

A representative TEM micrograph corresponding to the TBN sample, which is depicted in Fig. 3(a), confirmed the heterogeneous particle size distribution observed by SEM. An ED study established the notion that the larger particles in the micrometric range corresponded to the  $\text{TiB}_2$  phase (marked in the image) with a hexagonal symmetry and  $P6/mmm$  space group (191). The corresponding ED pattern was oriented along the  $[101]$  zone axis and is presented in Fig 3(a). Some of the medium crystalline diffraction domains (in the submicrometric range) corresponded to the  $\text{TiB}$  phase ( $[031]$  zone axis depicted) with an orthorhombic symmetry and  $Pnma$  space group (62). Other medium-sized crystals belonged to the  $\text{TiN}$  phase ( $[100]$  zone axis is presented) with a cubic symmetry and  $Fm\bar{3}m$  space group (225). The smallest particles in the nanometric range that surrounded the  $\text{TiB}_2$  particles also corresponded to the  $\text{TiN}$  phase. When an electron beam was diffracted along an area, such as the area that is circled in the image that contained these small diffraction domains, ED ring patterns were observed.

The EELS experiments performed using the TBN composite confirmed the presence of the three different phases; the characteristic spectra for  $\text{TiB}_2$ ,  $\text{TiB}$ , and  $\text{TiN}$  are presented in Fig. 4.  $B-K$  and  $Ti-L_{2,3}$  edges were recorded in the  $\text{TiB}_2$  and  $\text{TiB}$  phases, and  $N-K$  and  $Ti-L_{2,3}$  edges were recorded in the  $\text{TiN}$  phase. It is worth mentioning that the  $Ti-L_{2,3}$  edge displayed the same shape in the  $\text{TiB}_2$  and  $\text{TiB}$  phases; however, it showed a slightly different shape (marked with arrows) when it was recorded in the  $\text{TiN}$  phase. This was due to the  $Ti$  bonds that are similar in  $\text{TiB}_2$  and  $\text{TiB}$ , which differ from those found in  $\text{TiN}$ . A semi-quantitative analysis was conducted in the  $\text{TiB}_2$  and  $\text{TiB}$  phases, and the calculated  $Ti : B$  ratio was verified to conform to the  $2 : 1$  and  $1 : 1$  stoichiometries, respectively.

The micrograph presented in Fig. 3(b) corresponds to the TBC composite; a heterogeneous particle size distribution was observed. The largest crystalline domains belonged to the  $\text{TiB}_2$  phase. The marked crystal was oriented along the

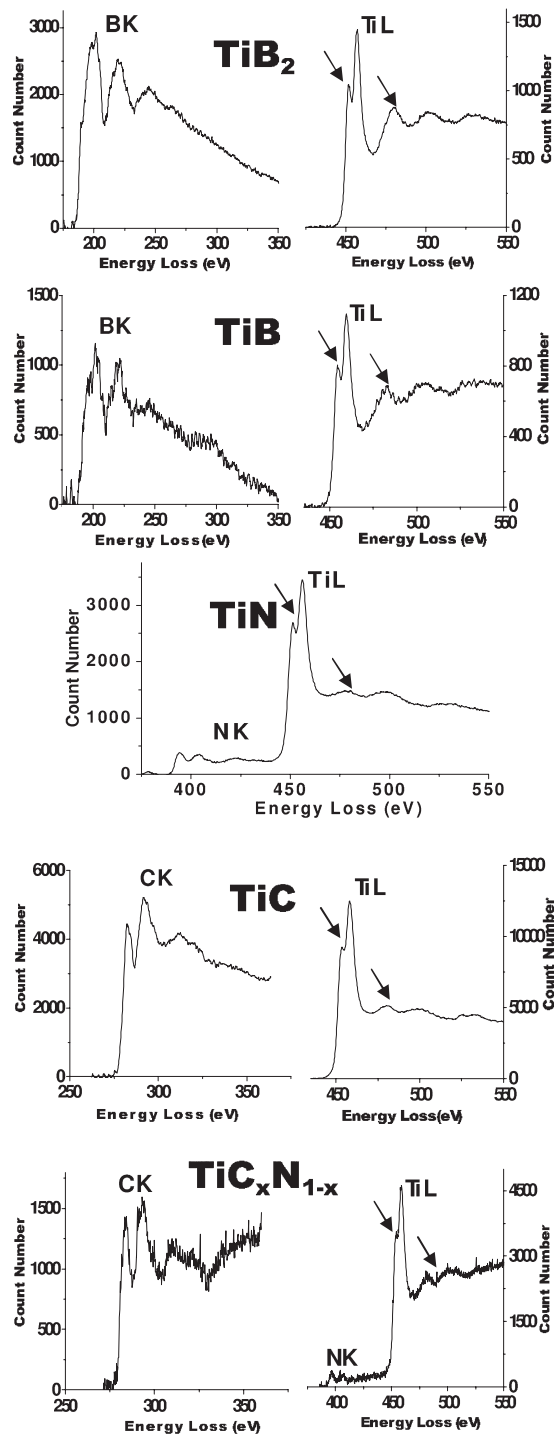


Fig. 4. EELS representative spectra obtained for  $\text{TiB}_2$ ,  $\text{TiB}$ ,  $\text{TiN}$ ,  $\text{TiC}$ , and  $\text{TiC}_x\text{N}_{1-x}$  phases in the TBN, TBC, and TBCN ceramic composites.

$[001]$  zone axis, and its ED pattern is depicted in Fig. 3(b). The area marked with a circle, in which submicrometric and nanometric crystallites were observed, corresponded to the  $\text{TiC}$  phase, as derived from the ED ring pattern [Fig. 3(b)]. Representative EELS spectra are presented in Fig. 4.  $B-K$  and  $Ti-L_{2,3}$  edges were recorded in the  $\text{TiB}_2$  phase, and  $C-K$  and  $Ti-L_{2,3}$  edges were recorded in the  $\text{TiC}$  phase. The shapes of the  $Ti-L_{2,3}$  edges appearing in both phases were different (marked with arrows); this difference was greater than the  $Ti-L_{2,3}$  edge from the  $\text{TiN}$  phase.

Microscopic characterizations of the TBCN composite are presented in Fig. 3(c), confirming the presence of two phases,  $\text{TiB}_2$  and  $\text{TiC}_x\text{N}_{1-x}$ . As in the two previous composites, the

TiB<sub>2</sub> phase showed quite large diffraction domains, which can be seen in the micrograph [Fig. 3(c)], with the corresponding ED pattern along the [001] zone axis. The smaller crystallites corresponded to the TiC<sub>x</sub>N<sub>1-x</sub> solid solution, and dispersion in the diffraction domain size was observed, as confirmed by the fact that dot-ED [the upper left side of Fig. 3(c)] and ring-ED [the lower right side of Fig. 3(c)] patterns were observed for this phase. The EELS spectra recorded for different crystals showed that the presence of a C-K edge was always associated with N-K and Ti-L<sub>2,3</sub> edges (Fig. 4), confirming the formation of a TiC<sub>x</sub>N<sub>1-x</sub> solid solution phase. In summary, the microstructural characterization of the three ceramic composite powders revealed that the TiB<sub>2</sub> phase was always obtained with a particle size larger than the sizes of the other constituents of the composites, i.e., TiN, TiC, or TiC<sub>x</sub>N<sub>1-x</sub>, which were usually on the nanometer scale. These results are consistent with the XRD diagrams of Fig. 1, which show broader reflections for the TiN, TiC, and TiC<sub>x</sub>N<sub>1-x</sub> phases compared with those corresponding to the TiB<sub>2</sub> phase.

Table II shows a new set of reactant mixtures, which corresponds to some variations of the TBN, TBC, and TBCN composite samples from Table I. These milling experiments were designed to verify the ability of the MSR process to tailor the chemical composition of the final product. The XRD diagrams of the TBN family samples are shown in Fig. 5, which clearly shows that the relative amounts of TiB<sub>2</sub> and TiN can be modulated simply by modifying the initial Ti/B atomic ratio. These findings were confirmed by quantification using the Rietveld refinement (Table II). Moreover, the  $t_{ig}$  values in Table II show how the ignition time increased with decreasing relative amounts of boron in the starting mixture and illustrate the importance of the presence of boron to induce ignition. This trend is a direct consequence of the increasing difficulty of igniting elemental mixtures, in which the extent of the self-sustaining reaction between titanium and nitrogen becomes increasingly important. At the same time, the amount of TiB in the final product, as a consequence of the incomplete reaction between titanium and nitrogen, increased with the decrease in boron content. TiB was not detected in the mixture with a Ti/B atomic ratio of 2/3. In any case, TiB always appeared as a secondary phase, the maximum amount of which was 15 wt% in the less favorable mixture, with a Ti/B atomic ratio of 2/1.

Figure 6, which shows the variations in the TBC series, clearly demonstrates how modifying the boron and carbon ratio in the starting mixture gives rise to composite materials with different relative amounts of the TiB<sub>2</sub> and TiC constituent

phases, which was confirmed by quantification using the Rietveld refinement (Table II).

Finally, Fig. 7 and Table II show the compositional variations performed in the TBCN series. The ignition time values in Table II show two trends. On one hand, ignition occurred at shorter times as the relative amount of boron in the starting mixture was increased, in line with previous results demonstrating the importance of the presence of boron to induce the ignition of the mixtures. On the other hand, for the same Ti/B ratio, the ignition time was further reduced when the relative amount of graphite was decreased. In a previous study on the synthesis of transition metal carbonitrides by the MSR process, the ignition of the reactant mixture was determined by the synergistic effect of nitrogen and carbon.<sup>41</sup> Although the presence of carbon was important to self-sustain the reaction, and a minimal amount of carbon was always necessary, the ignition of the mixture was favored by the presence of nitrogen.

It is worth noting that in this TBCN series, the MSR procedure allowed us to modify both the molar proportions of the TiB<sub>2</sub> and TiC<sub>x</sub>N<sub>1-x</sub> constituent phases (Table II) as well as the chemical composition of the TiC<sub>x</sub>N<sub>1-x</sub> solid solution by an appropriate adjustment of the reactants' ratio. The relative amounts of the TiB<sub>2</sub> and TiC<sub>x</sub>N<sub>1-x</sub> phases in the final product were fixed by both the Ti/(B+C) and B/C atomic ratios. All boron were consumed to form TiB<sub>2</sub>, and the remaining Ti reacted simultaneously with graphite and the nitrogen atmosphere to produce TiC<sub>x</sub>N<sub>1-x</sub>. The stoichiometry of the solid solution was controlled by the ratio (Ti-1/2B)/C. This is illustrated in the inset of Fig. 7 for samples TBCN-c, TBCN, and TBCN-d, which shows a shift in the (111) and (200) reflections of the TiC<sub>x</sub>N<sub>1-x</sub> phase; this shift was attributed to the different C/N ratios in the solid solution. The lattice parameter of TiC<sub>x</sub>N<sub>1-x</sub> was calculated from the XRD diagrams, and values of 4.304, 4.292, and 4.279 Å were obtained for samples TBCN-c, TBCN, and TBCN-d, respectively. These values are in accordance with the final TiC<sub>x</sub>N<sub>1-x</sub> stoichiometry and are close to the value expected from the atomic ratio of the starting mixture.<sup>23</sup> The presence of TiB in some products slightly enriched the carbon content of the carbonitride phase. The presence of TiB in this TBCN series in samples with higher Ti/(B+C) starting ratios was due, as in the previous TBN series, to an incomplete reaction of Ti with nitrogen to form, in this case, the TiC<sub>x</sub>N<sub>1-x</sub> phase.

The overall results shown in Table II indicate that TiB tended to form when the Ti/(B+C) atomic ratio was ~1 or higher. This was due to the difficulty of completing the

**Table II. Elemental Mixtures Corresponding to Variations of the Composite Materials in Table I, Modifying the Initial Atomic Ratio of the Reactants and Indicating the Used Atmosphere, the Ignition Time ( $t_{ig}$ ) of the MSR Process, and the Phase Quantification in the Products, as Calculated by the Rietveld Refinement with Goodness of Fit ( $\chi^2$ ).**

Sample	Solid Reactants (atomic ratio)	Atmosphere	$t_{ig}$ (min)	Phase Content (wt%)	$\chi^2$
TBN-a	Ti + B (2/3)	N <sub>2</sub>	35	TiB <sub>2</sub> /TiN/TiB 73/27/0	2.5
TBN-b	Ti + B (3/4)		40	TiB <sub>2</sub> /TiN/TiB 66/30/4	4.6
TBN	Ti + B (1/1)		57	TiB <sub>2</sub> /TiN/TiB 47/39/14	2.0
TBN-c	Ti + B (3/2)		102	TiB <sub>2</sub> /TiN/TiB 35/58/7	4.1
TBN-d	Ti + B (2/1)		147	TiB <sub>2</sub> /TiN/TiB 19/66/15	4.6
TBC-a	Ti + B + C (3/4/1)	He	44	TiB <sub>2</sub> /TiC 66/34	4.2
TBC	Ti + B + C (2/2/1)		55	TiB <sub>2</sub> /TiC 51/49	4.7
TBC-b	Ti + B + C (3/2/2)		55	TiB <sub>2</sub> /TiC 36/64	4.2
TBCN-a	Ti + B + C (3/4/0.7)	N <sub>2</sub>	36	TiB <sub>2</sub> /TiC <sub>x</sub> N <sub>1-x</sub> /TiB 63/37/0	3.1
TBCN-b	Ti + B + C (3/4/0.3)		22	TiB <sub>2</sub> /TiC <sub>x</sub> N <sub>1-x</sub> /TiB 64/36/0	5.3
TBCN-c	Ti + B + C (2/2/0.7)		43	TiB <sub>2</sub> /TiC <sub>x</sub> N <sub>1-x</sub> /TiB 51/49/0	3.5
TBCN	Ti + B + C (2/2/0.5)		44	TiB <sub>2</sub> /TiC <sub>x</sub> N <sub>1-x</sub> /TiB 50/50/0	3.2
TBCN-d	Ti + B + C (2/2/0.3)		31	TiB <sub>2</sub> /TiC <sub>x</sub> N <sub>1-x</sub> /TiB 49/48/3	4.0
TBCN-e	Ti + B + C (3/2/1.4)		45	TiB <sub>2</sub> /TiC <sub>x</sub> N <sub>1-x</sub> /TiB 36/64/0	2.6
TBCN-f	Ti + B + C (3/2/0.6)		40	TiB <sub>2</sub> /TiC <sub>x</sub> N <sub>1-x</sub> /TiB 27/63/10	3.9

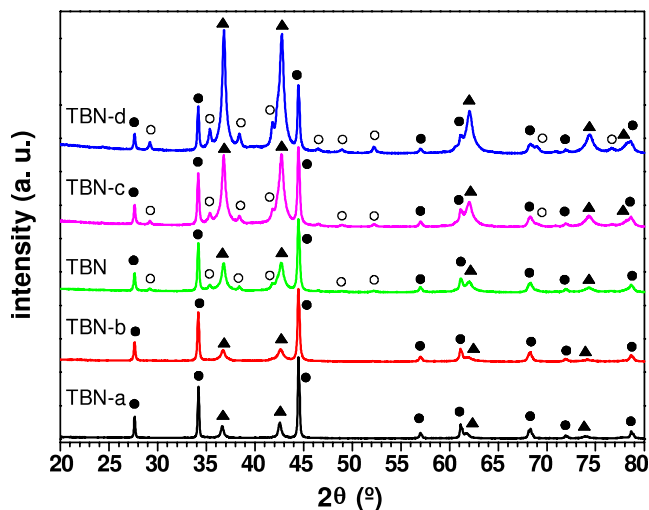


Fig. 5. X-ray powder diffraction diagrams of the products obtained from the MSR process for the TBN series. (●)  $\text{TiB}_2$ ; (▲)  $\text{TiN}$ ; (○)  $\text{TiB}$ .

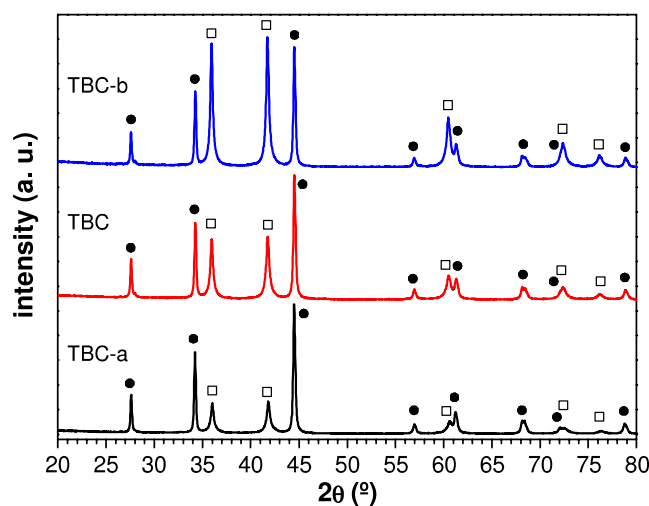


Fig. 6. X-ray powder diffraction diagrams of the products obtained from the MSR process for the TBC series. (●)  $\text{TiB}_2$ ; (□)  $\text{TiC}$ .

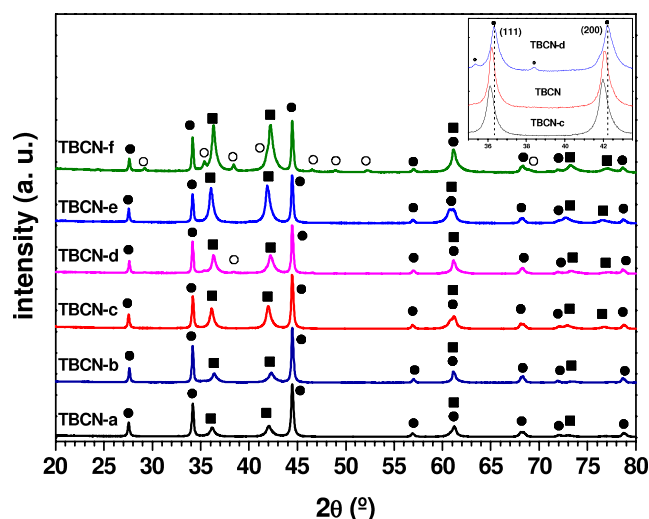
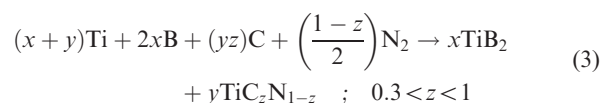
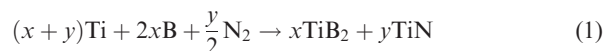


Fig. 7. X-ray powder diffraction diagrams of the products obtained from the MSR process for the TBCN series. (●)  $\text{TiB}_2$ ; (■)  $\text{TiC}_x\text{N}_{1-x}$ ; (○)  $\text{TiB}$ . In the inset, the (111) and (200) reflections of the  $\text{TiC}_x\text{N}_{1-x}$  phase in samples TBCN-c, TBCN, and TBCN-d are shown, illustrating the shift due to a different C/N ratio.

self-sustaining solid-gas reactions induced by milling, which resulted in a lower incorporation of nitrogen into the final product than was required to obtain stoichiometric  $\text{TiB}_2$ – $\text{TiN}$  and  $\text{TiB}_2$ – $\text{TiC}_x\text{N}_{1-x}$  mixtures. In any case,  $\text{TiB}$  was the only secondary phase detected, and it should be noted that this phase is also an interesting refractory compound with properties similar to those of  $\text{TiB}_2$ .<sup>42–44</sup> Moreover, the formation of  $\text{TiB}$  prevented the presence of unreacted  $\text{Ti}$  in the ceramic composite, which would have been detrimental to the final properties of the material.

In summary, the MSR procedure represents an alternative procedure for obtaining composite materials in the  $\text{Ti}$ – $\text{B}$ – $\text{C}$ – $\text{N}$  system with great control over the composition of the final product. According to the results shown in Table II, the overall chemical reactions associated with the MSR processes studied in this work were derived and are as follows:



#### IV. Conclusions

The experimental results in this work show that the MSR process can be very useful for the synthesis of multiphase materials. Powdered ceramic composites composed of  $\text{TiB}_2$ , and  $\text{TiC}$ ,  $\text{TiN}$ , or  $\text{TiC}_x\text{N}_{1-x}$  were prepared in a single step from the constituent elements in a controlled atmosphere. The ability of the MSR to tailor the chemical composition of composite materials belonging to the  $\text{Ti}$ – $\text{B}$ – $\text{C}$ – $\text{N}$  system was demonstrated, and a broad range of compositions was obtained. The composition of the ceramic composite powders was designed by carefully adjusting the atomic ratio of the solid reactants (titanium, boron, and carbon) and appropriately choosing the type of surrounding atmosphere, inert or reactive, employed during milling. The microstructural characterization of composite powders showed an excellent distribution of different components, which was mainly composed of  $\text{TiB}_2$  micrometric faceted particles surrounded by  $\text{TiC}$ ,  $\text{TiN}$ , or  $\text{TiC}_x\text{N}_{1-x}$  rounded particles in the submicrometric and nanometric ranges.

#### Acknowledgments

The authors wish to thank Ms. C. Gallardo for her assistance in the high-energy ball-milling experiments.

#### References

- R. Telle, L. S. Sigl, and K. Takagi, "Transition Metal Boride Ceramics"; pp. 803–945 in *Handbook of Ceramic Hard Materials*, Vol. 2. Edited by R. Riedel. Wiley-VCH, Weinheim, Germany, 2000.
- H. O. Pierson, *Handbook of Refractory Carbides and Nitrides*. Noyes Publications, Westwood, NJ, 1996.
- L. Wang, M. R. Wixom, and L. T. Thompson, "Structural and Mechanical Properties of  $\text{TiB}_2$  and  $\text{TiC}$  Prepared by Self-Propagating High Temperature Synthesis/Dynamic Compaction," *J. Mater. Sci.*, **29**, 534–43 (1994).
- H. Pastor, "Titanium-Carbonitride-Based Hard Alloys for Cutting Tools," *Mater. Sci. Eng., A*, **106**, 401–9 (1988).
- G. Wen, S. B. Li, B. S. Zhang, and Z. X. Guo, "Reaction Synthesis of  $\text{TiB}_2$ – $\text{TiC}$  Composites With Enhanced Toughness," *Acta Mater.*, **49**, 1463–70 (2001).
- D. Vallauri, I. C. Atías Adrián, and A. Chrysanthou, "TiC– $\text{TiB}_2$  Composites: A Review of Phase Relationships, Processing and Properties," *J. Eur. Ceram. Soc.*, **28**, 1697–713 (2008).
- X. Zhou, S. Zhang, M. Zhu, and B. Chen, "Investigation of  $\text{TiB}_2$ – $\text{TiC}$  Composites Produced by SHS and Their Application in Hall-Heroult Cells for Aluminum Electrolysis," *Int. J. Self-Prop. High-Temp. Synth.*, **7**, 403–8 (1998).

- <sup>8</sup>D. Brodtkin, S. Kalidindi, M. Barsoum, and A. Zavaliangos, "Microstructural Evolution During Transient Plastic Phase Processing of Titanium Carbide-Titanium Boride Composites," *J. Am. Ceram. Soc.*, **79**, 1945–52 (1996).
- <sup>9</sup>T. Watanabe, T. Doutsu, and T. Nakanishi, "Sintering Properties and Cutting-Tool Performance of Ti(C,N)-Based Ceramics," *Key Eng. Mater.*, **114**, 189–266 (1996).
- <sup>10</sup>D. Vallauri, B. DeBenedetti, L. Jaworska, P. Klimczyk, and M. A. Rodriguez, "Wear-Resistant Ceramic and Metal-Ceramic Ultrafine Composites Fabricated from Combustion Synthesized Metastable Powders," *Int. J. Refract. Met. Hard Mater.*, **27**, 996–1003 (2009).
- <sup>11</sup>C. Musa, A. M. Locci, R. Licheri, R. Orrù, G. Cao, D. Vallauri, F. A. Deorsola, E. Tresso, J. Suffner, H. Hahn, P. Klimczyk, and L. Jaworska, "Spark Plasma Sintering of Self-Propagating High-Temperature Synthesized TiC<sub>0.7</sub>/TiB<sub>2</sub> Powders and Detailed Characterization of Dense Product," *Ceram. Int.*, **35**, 2587–99 (2009).
- <sup>12</sup>H. Kaya, "The Application of Ceramic-Matrix Composites to the Automotive Ceramic Gas Turbine," *Compos. Sci. Technol.*, **59**, 861–72 (1999).
- <sup>13</sup>R. Ren, Z. Yang, and L. L. Shaw, "Nanostructured TiN Powder Prepared via an Integrated Mechanical and Thermal Activation," *Mater. Sci. Eng., A*, **286**, 65–71 (2000).
- <sup>14</sup>C. Subramanian, T. Murthy, and A. K. Suri, "Synthesis and Consolidation of Titanium Diboride," *Int. J. Refract. Met. Hard Mater.*, **25**, 345–50 (2007).
- <sup>15</sup>J. Xiang, Z. Xie, Y. Huang, and H. Xiao, "Synthesis of Ti(C,N) Ultrafine Powders by Carbothermal Reduction of TiO<sub>2</sub> Derived from sol-gel Process," *J. Eur. Ceram. Soc.*, **20**, 933–8 (2000).
- <sup>16</sup>S. G. Ko, C. W. Won, B. S. Chun, and H. Y. Sohn, "The Self-Propagating High-Temperature Synthesis (SHS) of Ultrafine High-Purity TiC Powder from TiO<sub>2</sub>+Mg+C," *J. Mat. Sci.*, **30**, 2835–7 (1995).
- <sup>17</sup>D. D. Radev and M. Marinov, "Properties of Titanium and Zirconium Diborides Obtained by Self-Propagated High-Temperature Synthesis," *J. Alloys Compd.*, **244**, 48–51 (1996).
- <sup>18</sup>D. Carole, N. Fréty, S. Paris, D. Vrel, F. Bernard, and R. M. Marin-Ayral, "Investigation of the SHS Mechanisms of Titanium Nitride by *in Situ* Time-Resolved Diffraction and Infrared Thermography," *J. Alloys Compd.*, **436**, 181–6 (2007).
- <sup>19</sup>C. L. Yeh and Y. D. Chen, "Direct Formation of Titanium Carbonitrides by SHS in Nitrogen," *Ceram. Int.*, **31**, 719–29 (2005).
- <sup>20</sup>L. Takacs, "Self-Sustaining Reactions Induced by Ball Milling," *Progr. Mater. Sci.*, **47**, 355–414 (2002).
- <sup>21</sup>D. D. Radev and D. Klissurski, "Mechanochemical Synthesis and SHS of Diborides of Titanium and Zirconium," *J. Mater. Synth. Process.*, **9**, 131–6 (2001).
- <sup>22</sup>B. H. Lohse, A. Calka, and D. Wexler, "Effect of Starting Composition on the Synthesis of Nanocrystalline TiC During Milling of Titanium and Carbon," *J. Alloys Compd.*, **394**, 148–51 (2005).
- <sup>23</sup>J. M. Córdoba, M. J. Sayagués, M. D. Alcalá, and F. J. Gotor, "Synthesis of Titanium Carbonitride Phases by Reactive Milling of the Elemental Mixed Powders," *J. Am. Ceram. Soc.*, **88**, 1760–4 (2005).
- <sup>24</sup>I. Gotman, N. A. Travitzky, and E. Y. Gutmanas, "Dense *in Situ* TiB<sub>2</sub>/TiN and TiB<sub>2</sub>/TiC Ceramic Matrix Composites: Reactive Synthesis and Properties," *Mater. Sci. Eng., A*, **244**, 127–37 (1998).
- <sup>25</sup>L. Klinger, I. Gotman, and D. Horvitz, "In Situ Processing of TiB<sub>2</sub>/TiC Ceramic Composites by Thermal Explosion Under Pressure: Experimental Study and Modelling," *Mat. Sci. Eng. A*, **302**, 92–9 (2001).
- <sup>26</sup>L. Zhan, P. Shen, Y. Yang, J. Zhang, and Q. Jiang, "Self-Propagating High-Temperature Synthesis of TiC<sub>x</sub>N<sub>y</sub>-TiB<sub>2</sub> Ceramics from a Ti-B<sub>4</sub>C-BN System," *Int. J. Refract. Met. Hard Mater.*, **27**, 829–34 (2009).
- <sup>27</sup>G. Liu, J. Li, X. Ning, and Y. Chen, "Combustion Synthesis of TiC<sub>x</sub>N<sub>1-x</sub>-TiB<sub>2</sub> Ceramic Composites in a High-Gravity Field," *Mat. Res. Bull.*, **46**, 958–61 (2011).
- <sup>28</sup>R. Tomoshige, A. Murayama, and T. Masushita, "Production of TiB<sub>2</sub>-TiN Composites by Combustion Synthesis and Their Properties," *J. Am. Ceram. Soc.*, **80**, 761–4 (1997).
- <sup>29</sup>C. L. Yeh and G. S. Teng, "Combustion Synthesis of TiN-TiB<sub>2</sub> Composites in Ti/BN/N<sub>2</sub> and Ti/BN/B Reaction Systems," *J. Alloys Compd.*, **424**, 152–8 (2006).
- <sup>30</sup>A. M. Locci, R. Orru, G. Cao, and Z. A. Munir, "Simultaneous Spark Plasma Synthesis and Densification of TiC-TiB<sub>2</sub> Composites," *J. Am. Ceram. Soc.*, **89**, 848–55 (2006).
- <sup>31</sup>C. L. Yeh and Y. L. Chen, "Combustion Synthesis of TiC-TiB<sub>2</sub> Composites," *J. Alloys Compd.*, **463**, 373–7 (2008).
- <sup>32</sup>J. W. Lee, Z. A. Munir, and M. Ohyanagi, "Dense Nanocrystalline TiB<sub>2</sub>-TiC Composites Formed by Field Activation from High-Energy Ball Milled Reactants," *Mat. Sci. Eng. A*, **325**, 221–7 (2002).
- <sup>33</sup>J. Li, F. Li, K. Hu, and Y. Zhou, "TiB<sub>2</sub>/TiC Nanocomposite Powder Fabricated via High Energy Ball Milling," *J. Eur. Ceram. Soc.*, **21**, 2829–33 (2001).
- <sup>34</sup>J. H. Shim, J. S. Byun, and Y. W. Cho, "Mechanochemical Synthesis of Nanocrystalline TiN/TiB<sub>2</sub> Composite Powder," *Scrip. Mater.*, **47**, 493–7 (2002).
- <sup>35</sup>A. M. Locci, R. Orru, G. Cao, and Z. A. Munir, "Effect of Ball Milling on Simultaneous Spark Plasma Synthesis and Densification of TiC-TiB<sub>2</sub> Composites," *Mat. Sci. Eng., A*, **434**, 23–9 (2006).
- <sup>36</sup>L. X. Qiu, B. Yao, Z. H. Ding, Y. J. Zheng, X. P. Jia, and W. T. Zheng, "Characterization of Structure and Properties of TiN-TiB<sub>2</sub> Nano-Composite Prepared by Ball Milling and High Pressure Heat Treatment," *J. Alloys Compd.*, **456**, 436–40 (2008).
- <sup>37</sup>J. Rodriguez-Carvajal, "Recent Developments of the Program Fullprof" in Commission on Powder Diffraction (IUCr), *Newsletter*, **26**, 12–9 (2001).
- <sup>38</sup>M. Binnewies and E. Milke, *Thermochemical Data of Elements and Compounds*. Wiley-VCH, Germany, 1999.
- <sup>39</sup>L. Zhan, P. Shen, and Q. Jiang, "Effect of Nickel Addition on the Exothermic Reaction of the Ti-C-BN System," *Int. J. Refract. Met. Hard Mater.*, **28**, 324–9 (2010).
- <sup>40</sup>F. J. Gotor, M. D. Alcalá, C. Real, and J. M. Criado, "Combustion Synthesis of TiN Induced by High-Energy Ball Milling of Ti Under Nitrogen Atmosphere," *J. Mater. Res.*, **17**, 1655–63 (2002).
- <sup>41</sup>J. M. Córdoba, M. J. Sayagués, M. D. Alcalá, and F. J. Gotor, "Monophasic Nanostructured Powders of Niobium, Tantalum, and Hafnium Carbonitrides Synthesized by a Mechanically Induced Self-Propagating Reaction," *J. Am. Ceram. Soc.*, **90**, 381–7 (2007).
- <sup>42</sup>S. Nakane, Y. Takano, M. Yoshinaka, K. Hirota, and O. Yamaguchi, "Fabrication and Mechanical Properties of Titanium Boride Ceramics," *J. Am. Ceram. Soc.*, **82**, 1627–8 (1999).
- <sup>43</sup>S. Madtha, C. Lee, and K. S. Ravi Chandran, "Physical and Mechanical Properties of Nanostructured Titanium Boride (TiB) Ceramic," *J. Am. Ceram. Soc.*, **91**, 1319–21 (2008).
- <sup>44</sup>S. Madtha and K. S. Ravi Chandran, "Reactive-Sinter-Processing and Attractive Mechanical Properties of Bulk and Nanostructured Titanium Boride," *J. Am. Ceram. Soc.*, **95**, 117–25 (2012). □